Supporting Information

3D Porous cementitious electrolyte with "stream-reservoir" ionic channels for high multifunctional performance structural supercapacitors

*Muyang Shi, Dong Zhang**

Key Laboratory of Advanced Civil Engineering Materials, Ministry of Education,

School of Materials Science and Engineering, Tongji University, Shanghai 201804,

PR China

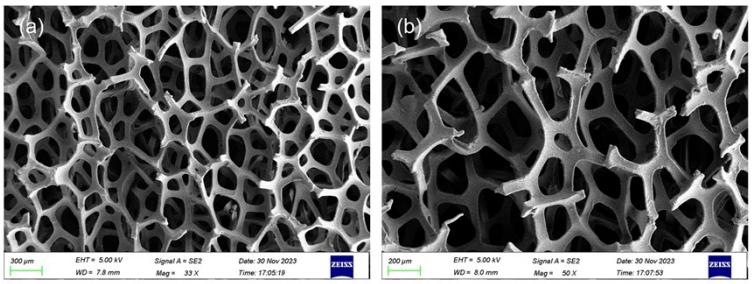

Figure S1. The SEM images of nickel foam.

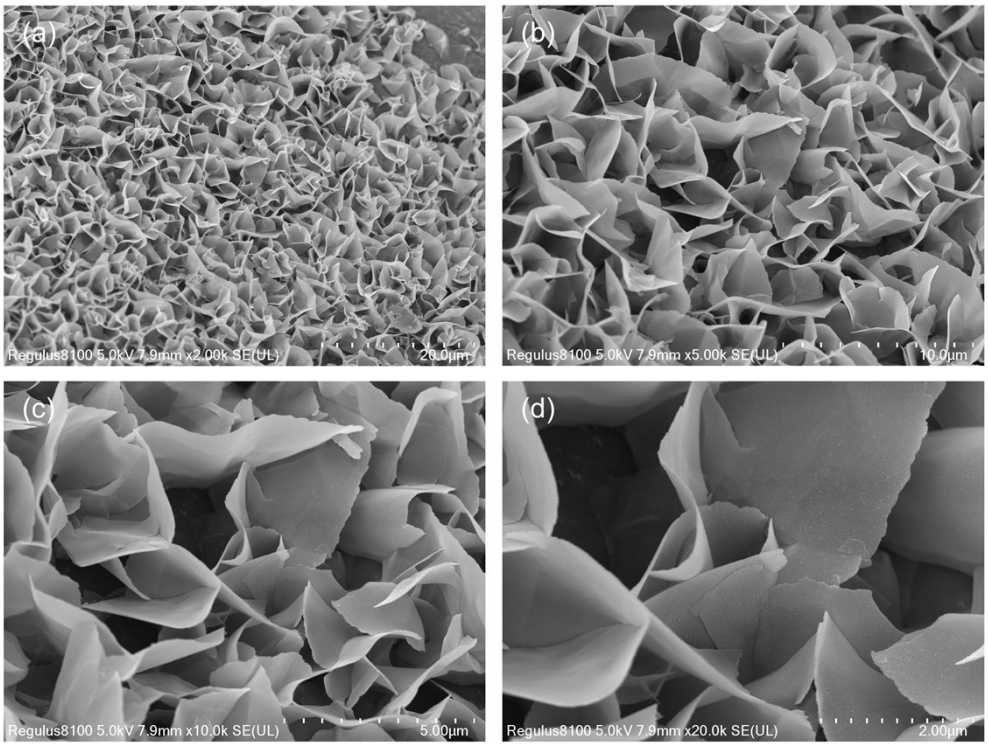

Figure S2. SEM images of rGO.

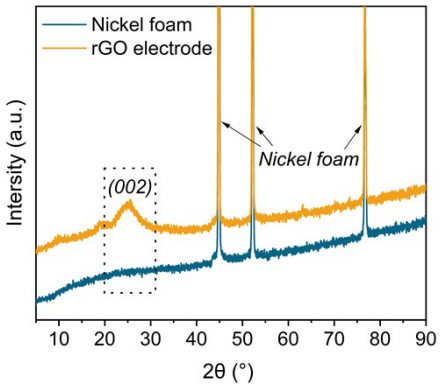

Figure S3. XRD patterns of the nickel foam and rGO electrodes.

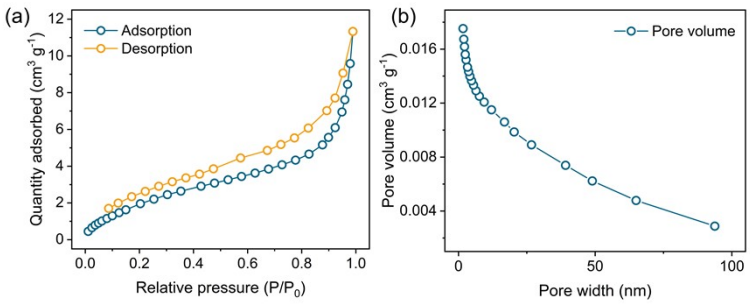

Figure S4. BET test of the rGO foam electrode. (a) N_2 adsorption/desorption isotherms. (b) corresponding pore size distributions.

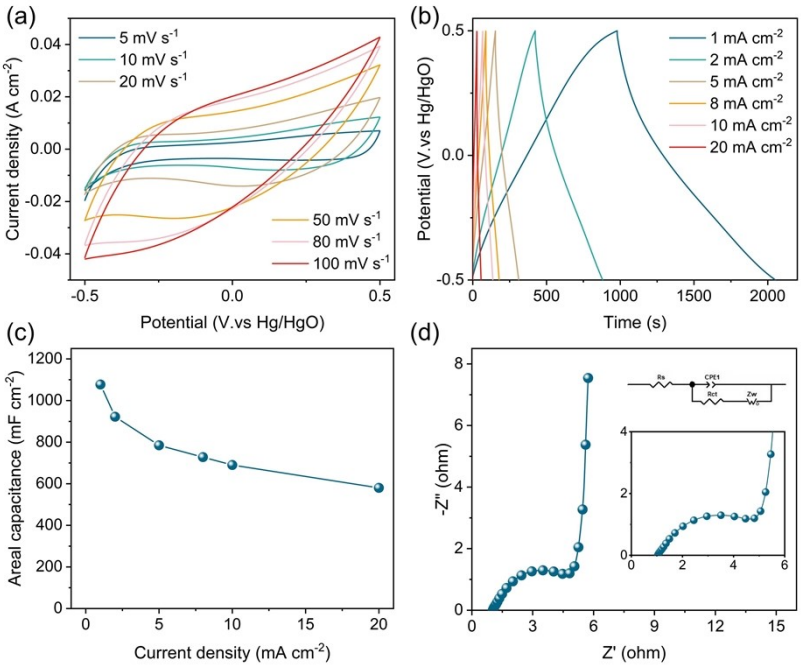

Figure S5. (a) CV curves at various scan rates and (b) GCD curves at various current densities for rGO. (c) The areal capacitance of rGO under various current densities. (d) Nyquist plots of rGO.

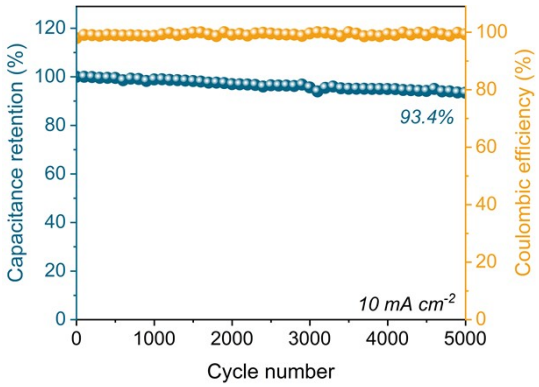

Figure S6. Cyclic performance of the rGO.

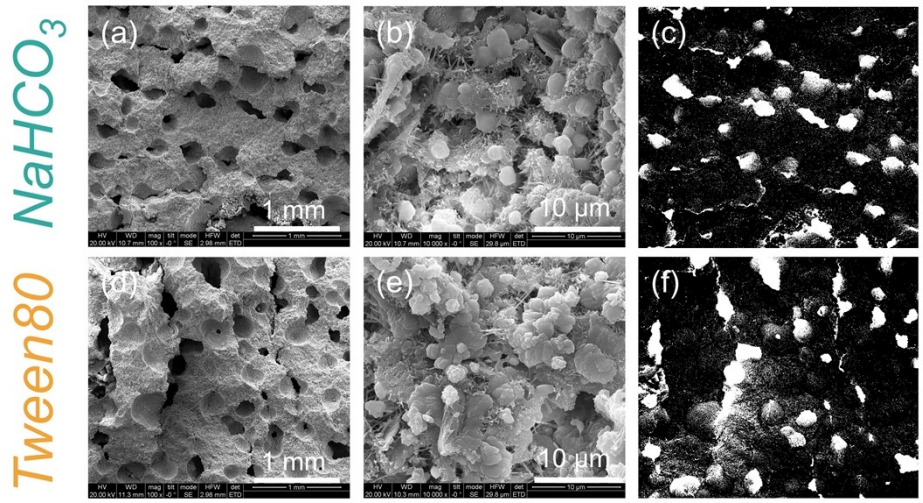

Figure S7. High and low magnifications of SEM images of cementitious electrolytes showing (a, b) $NaHCO_3$-PCE and (d, e) Tween80-PCE. Processing SEM images of cementitious electrolytes with different foaming agent types: (c) $NaHCO_3$-PCE and (f) Tween80-PCE.

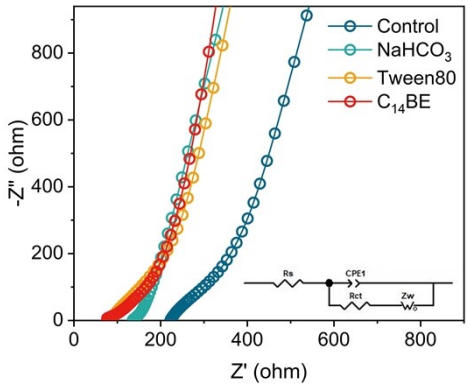

Figure S8. EIS curves of control/$NaHCO_3$/Tween80/C_{14}BE-PCE.

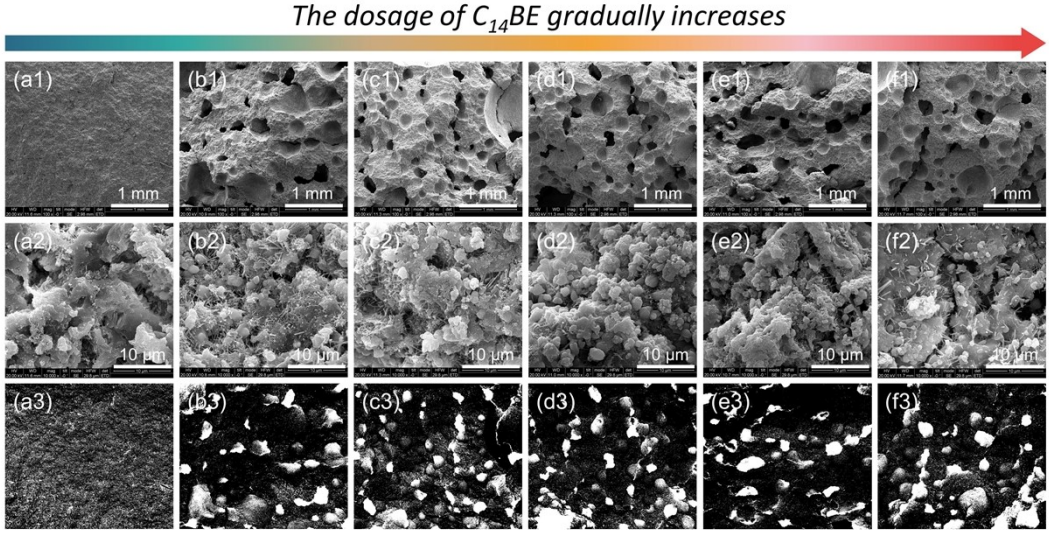

Figure S9. Low and high magnification SEM images of cementitious electrolytes with various contents of C_{14}BE: (a1, a2) 0 wt%; (b1, b2) 1 wt%; (c1, c2) 2 wt%; (d1, d2) 3 wt%; (e1, e2) 4 wt%; (f1, f2) 5 wt%. Processing SEM images of cementitious electrolytes with various contents of C_{14}BE: (a3) 0 wt%; (b3) 1 wt%; (c3) 2 wt%; (d3) 3 wt%; (e3) 4 wt%; (f3) 5 wt%.

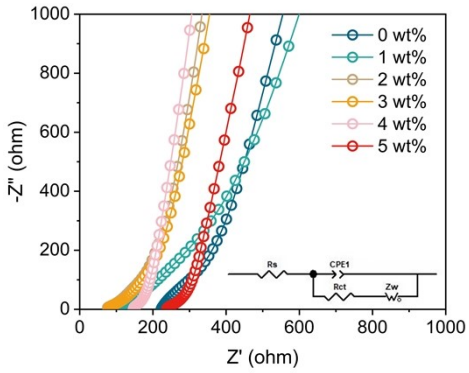

Figure S10. EIS curves of a series of C_{14}BE-PCE.

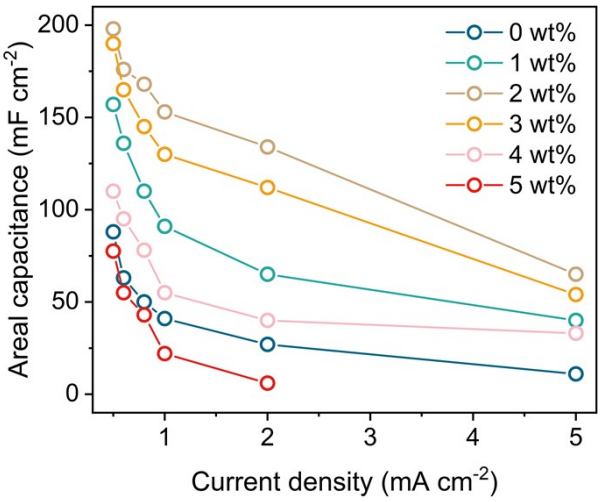

Figure S11. The areal capacitance of the different C_{14}BE-PCE-based SSCs under various current densities.

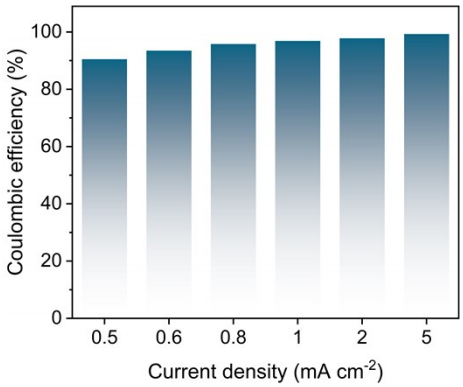

Figure S12. Coulombic efficiency of C_{14}BE-PCE-based redox-active SSC vs. the current density.

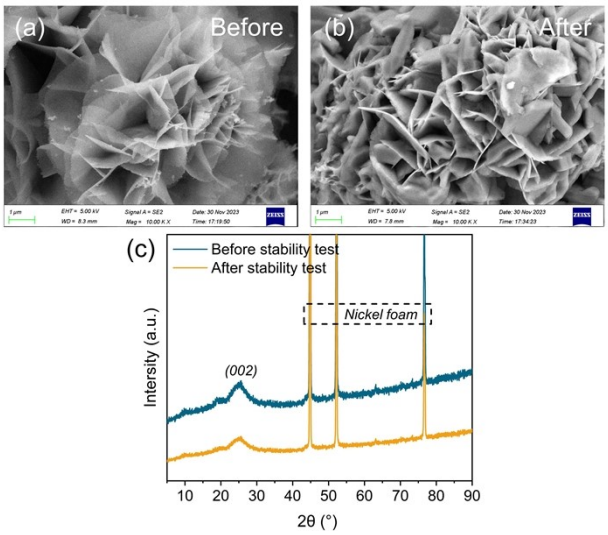

Figure S13. (a) The SEM image of rGO before cycling test. (b) The SEM image of rGO after cycling test. (c) XRD pattern of rGO before and after cycling test.

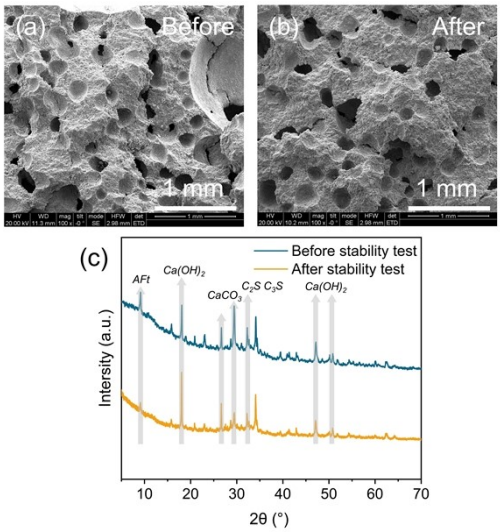

Figure S14. (a) The SEM image of C_{14}BE-PCE before cycling test. (b) The SEM image of C_{14}BE-PCE after cycling test. (c) XRD pattern of C_{14}BE-PCE before and after cycling test.

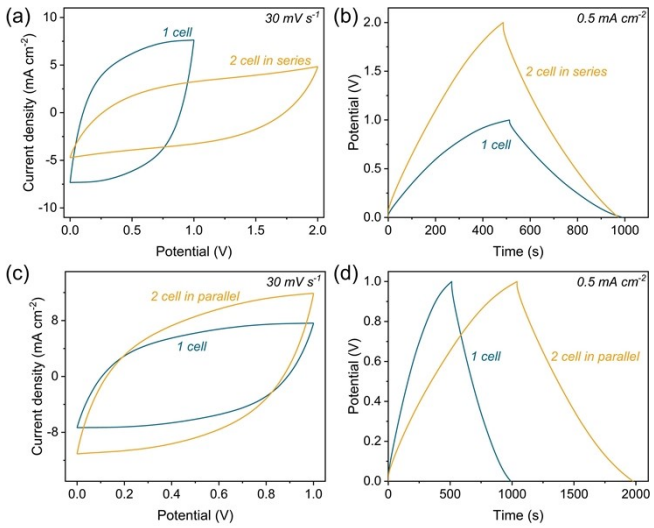

Figure S15. Electrochemical measurement on multiple SSCs connected in series and parallel. (a) CV profiles of one and two cells in series with a scan rate of 30 mV s^{-1}. (b) GCD curves of one and two cells in series with a current density of 0.5 mA cm^{-2}. (c) CV profiles of one and two cells in parallel with the scan rate of 30 mV s^{-1}. (d) GCD curves of one and two cells in parallel with a current density of 0.5 mA cm^{-2}.

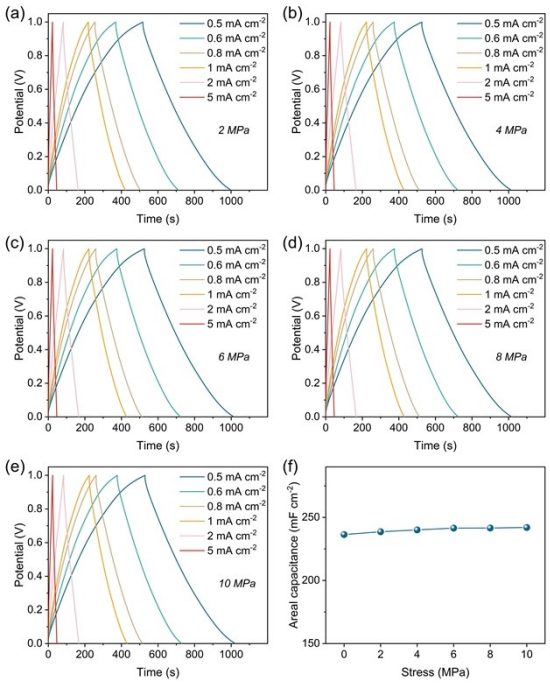

Figure S16. GCD curves of the C_{14}BE-PCE-based redox-active SSC at (a) 2 MPa, (b) 4 MPa, (c) 6 MPa, (d) 8 MPa, and (e) 10 MPa. (f) GCD comparison of the SSC at different stresses at a current density of 0.5 mA cm^{-2}.

Electrolyte composition	Ionic conductivity (mS cm^{-1})	Compressive strength (MPa)	Ref
polyMIPE	1.9	20	[1]
PEO-BMITFSI	0.1	0.4	[2]
Epoxy-$LiClO_4$	1.58	1.45	[3]
LATP- PVDF	1.64	14.2	[4]
PAA-aluminate cement	8.2	37.2	[5]
Portland cement	2.13	9.85	[6]
PVA-Portland cement	5.65	8.74	[7]
PEO-Portland cement	4.75	22.29	[8]
C_{14}BE-PCE	**13.1**	**29.5**	**This work**

Table S1. Comparison of solid electrolyte of previous studies and this work

References

1 V. Tu, L. E. Asp, N. Shirshova, F. Larsson, K. Runesson and R. Jänicke, Multifunct. Mater., 2020, **3**, 025001.
2 S. Leijonmarck, T. Carlson, G. Lindbergh, L. E. Asp, H. Maples and A. Bismarck, Composites Science and Technology, 2013, **89**, 149–157.
3 S.-H. Bae, C. Jeon, S. Oh, C.-G. Kim, M. Seo and I.-K. Oh, Carbon, 2018, **139**, 10–20.
4 Y. Jin, C. Liu, Z. Jia, X. Zong, D. Li, M. Fu, J. Wei and Y. Xiong, Journal of Alloys and Compounds, 2021, **874**, 159890.
5 J. X. Tu, X. X. Chen, X. B. Xiong, Y. Chen, J. Ma, H. Y. Cao and A. J. Li, Materials Today Chemistry, 2023, **28**, 101365.
6 J. Zhang, J. Xu and D. Zhang, J. Electrochem. Soc., 2016, **163**, E83–E87.
7 C. Xu and D. Zhang, Journal of Composite Materials, 2021, **55**, 1359–1369.
8 C. Fang and D. Zhang, Electrochimica Acta, 2022, **401**, 139491.